AGU PUBLICATIONS

Water Resources Research

RESEARCH ARTICLE
10.1002/2013WR014468

Key Points:
- Parameterization schemes of surface energy fluxes are simplified
- Surface energy fluxes are estimated without calculating resistances
- Fewer input variables are required

Correspondence to:
H. Tang,
hjtang@caas.cn

Citation:
Lu, J., R. Tang, H. Tang, and Z.-L. Li (2014), A new parameterization scheme for estimating surface energy fluxes with continuous surface temperature, air temperature, and surface net radiation measurements, *Water Resour. Res.*, *50*, 1245–1259, doi:10.1002/2013WR014468.

Received 25 JUL 2013
Accepted 26 JAN 2014
Accepted article online 31 JAN 2014
Published online 14 FEB 2014

A new parameterization scheme for estimating surface energy fluxes with continuous surface temperature, air temperature, and surface net radiation measurements

Jing Lu[1,2,3], Ronglin Tang[1], Huajun Tang[4], and Zhao-Liang Li[3,4]

[1]State Key Laboratory of Resources and Environmental Information System, Institute of Geographic Sciences and Natural Resources Research, Chinese Academy of Sciences, Beijing, China, [2]University of Chinese Academy of Sciences, Beijing, China, [3]ICube, UdS, CNRS, Illkirch, France, [4]Key Laboratory of Agri-informatics, Ministry of Agriculture/Institute of Agricultural Resources and Regional Planning, Chinese Academy of Agricultural Sciences, Beijing, China

Abstract This study develops a method for estimating surface energy fluxes (surface sensible heat flux (*H*), latent heat flux (*LE*), and soil heat flux (*G*)) simultaneously from continuous observations of surface temperature (T_s), air temperature (T_a), and net radiation (R_n) without calculating various resistances. First, *H*, *LE*, and *G* are parameterized by some constant parameters that remain fairly invariant during a given day and some known functions related to T_s and T_a. Second, these constant parameters are solved by a minimization technique based on surface energy balance. Data from ground-based measurements at the Yucheng station were used to evaluate the performance of the developed method. Results show that the simplified parameterization schemes well reproduce *H*, *LE*, and *G* with a root mean square error (RMSE) of ~20 W/m^2 at the instantaneous time scale, and perform better at the daily scale. For the estimates of *H*, *LE*, and *G* using the known T_s, T_a, and R_n measured at the Yucheng station as inputs, the RMSE is ~60 W/m^2 at the instantaneous time scale and ~20 W/m^2 at the daily scale. The requirement of continuous observations throughout a day in the developed method could be met by remotely sensed data from geostationary meteorological satellites. Fewer input variables and the obviation of calculating various resistances give the method the potential to generate surface fluxes over a large area.

1. Introduction

As an important component in the surface energy balance and the water cycle, knowledge of evapotranspiration (ET) at regional scales is increasingly required in fields such as agriculture, climate, and hydrology [*Farahani et al.*, 2007; *Jung et al.*, 2010; *Lathuillière et al.*, 2012; *Seneviratne et al.*, 2006]. Satellite remote sensing provides an unprecedented opportunity for ET estimation at regional scales. Numerous models have been proposed to estimate ET by incorporating remotely sensed variables, including one-source models [*Bastiaanssen et al.*, 1998; *Su*, 2002], two-source models [*Long and Singh*, 2012; *Mu et al.*, 2011; *Norman et al.*, 1995], triangle/trapezoid-type models [*Jiang and Islam*, 1999; *Moran et al.*, 1994; *Tang et al.*, 2010], empirical models [*Jackson et al.*, 1977], and data assimilation method [*Caparrini et al.*, 2003]. The advantages and disadvantages of these ET models have been reviewed in the literature [*Courault et al.*, 2005; *Kalma et al.*, 2008; *Li et al.*, 2009; *Verstraeten et al.*, 2008; *Wang and Dickinson*, 2012].

In general, the empirical and semiempirical models are simple and convenient for ET estimates, but the determination of empirical relationships and relevant coefficients is mostly site-specific [*Nagler et al.*, 2005; *Seguin and Itier*, 1983] or dependent on the domain size and spatial resolution of satellite images [*Long et al.*, 2012; *Tang et al.*, 2013a]. The physically based models can well depict the mechanism of water and heat flux transfer, but more surface and atmosphere variables, e.g., wind speed and roughness lengths for momentum and heat transfer, are needed to calculate various resistances, e.g., aerodynamic resistance and surface resistance [*Tang et al.*, 2011]. Furthermore, because most models make use of instantaneous observations from satellite sensors, retrieval errors of surface variables will inevitably affect the ET estimation [*Li et al.*, 2013a]. Temporal variations of surface variables in measurements contain important information on surface fluxes, which could be used to improve satellite-based ET estimation at longer time scales [*Anderson et al.*, 1997; *Lu et al.*, 2013; *Stisen et al.*, 2008; *Wang et al.*, 2006]. The data assimilation method is an important alternative for the estimation of surface fluxes at continuous temporal and spatial scales [*Boni et al.*,

2001; *Xu et al*., 2011; *Sun et al*., 2011, 2012]. However, land surface models (LSMs) involved in the assimilation schemes require extensive atmospheric forcing and are generally computationally demanding, which may hamper a wider application of the method [*McLaughlin et al*., 2006].

Raffy and Becker [1985] developed an inverse method to estimate surface fluxes without a priori knowledge of heat transfer resistances by incorporating multiple observations of surface temperature, air temperature, incoming solar radiation, and wind speed in a day. The inverse method is fairly similar to the data assimilation technique, but some simple parameterization schemes replaced the complex LSMs in data assimilation systems. The key of the method of *Raffy and Becker* [1985] is to parameterize energy balance components as functions of some unknown constants and surface parameters/variables of surface temperature, air temperature, and wind speed. The flux minimization method and the temperature minimization method are used to solve for the unknown constants [*Abdellaoui et al*., 1986; *Raffy and Becker*, 1986]. After these unknown constants are solved, components in the energy balance equation can be obtained simultaneously.

For estimating surface energy fluxes without the calculation of various resistances, this study aims to develop simpler parameterizations for sensible, latent, and soil heat fluxes based on the method of *Raffy and Becker* [1985] using continous information of surface parameters. Differing from the method of *Raffy and Becker* [1985], the developed method entails several attributes: (1) the parameterization schemes of sensible, latent, and soil heat fluxes are simplified without using wind speed, roughness lengths, and other surface parameters, and only surface temperature and air temperature are used; and (2) the unknown constants are solved by the energy balance equation rather than the sophisticated heat conductivity equation. Principles of the developed parameterization schemes and procedures of deriving constant parameters will be detailed in section 2. Ground-based measurements at the Yucheng station in North China will be used to evaluate the performance of the parameterization schemes. Data will be described in section 3. Performance of the parameterization schemes and surface energy fluxes estimates based on energy balance will be investigated and discussed in section 4. Summary and conclusions are given in section 5.

2. Methods

2.1. Parameterization for Sensible Heat Flux (H)

Under the assumptions of quasi-stationarity and negligible horizontal advection, H can be written as [*Brutsaert*, 1982]

$$H=\rho_a c_p C_{DH}^{z_a} u(T_{aero}-T_a) \tag{1}$$

where ρ_a is the density of air (kg/m^3), c_p is the heat capacity of air (J/kg·K), $C_{DH}^{z_a}$ is the bulk transfer coefficient for sensible heat with respect to a reference height z_a (m) (–), u is the wind speed (m/s), T_{aero} is the aerodynamic temperature (K), and T_a is the air temperature (K).

Blümel [1998] proposed an algorithm for estimating the temporal course of H from continuous surface temperature (T_s) measurements and one-time-of-day T_a observation. In this method, $C_{DH}^{z_a}$ in unstable stratification is parameterized using the bulk Richardson number rather than the Monin-Obukhov length, so the iteration process for the calculation of H can be obviated, i.e.,

$$H=\rho_a c_p C_{DHneutral}^{z_a} u\left\{(T_s-T_a)+\left[(10\xi^2+5\xi)(z_a-d_0)g/(\overline{\Theta}u^2)\right](T_s-T_a)^2\right\} \tag{2}$$

in which $C_{DHneutral}^{z_a}=k^2/\{\ln[(z_a-d_0)/z_{0m}]\ln[(z_a-d_0)/z_{0h}]\}$, and

$$\xi=\ln[(z_a-d_0)/z_{0m}]/\ln[(z_a-d_0)/z_{0h}]$$

where $C_{DHneutral}^{z_a}$ is the bulk transfer coefficient for neutral conditions (–); $\overline{\Theta}$ is the mean T_a (K); g is the gravitational acceleration (9.8 m/s^2); k is the von Karman constant (0.4); and d_0, z_{0m}, and z_{0h} are the displacement height, the roughness height for momentum transfer, and the roughness height for heat transfer, respectively (m). It should be clarified here that T_s in equation (2) is essentially the aerodynamic temperature

rather than the surface radiative temperature. However, T_{aero} is not an easily measured variable in reality. To estimate H conveniently, T_s from geostationary meteorological satellite was used in the study of *Blümel* [1998].

Because ρ_a, c_p, z_{0m}, z_{0h}, and $\overline{\Theta}$ over a day period can be assumed as fairly invariant, on the basis of the idea of *Raffy and Becker* [1985], equation (2) can be simplified as

$$H = d_1[(T_s - T_a)] + d_2[(T_s - T_a)^2] \tag{3}$$

with $d_1 \approx \rho_a c_p C^{z_a}_{DHneutral} u$ and $d_2 \approx \rho_a c_p C^{z_a}_{DHneutral} u(10\xi^2 + 5\xi)(z_a - d_0)g/(\overline{\Theta}u^2)$.

d_1 in W/(m^2·K) seems to be the bulk heat conductance for sensible heat transfer at neutral atmospheric conditions and $d_2(T_s - T_a)$ in W/(m^2·K) can be regarded as the extension of the heat conductance to non-neutral atmospheric conditions. In theory, d_1 and d_2 are mainly related to wind speed. Differing from T_{aero}, the surface radiative temperature T_s is a composite parameter reflecting surface heat status, and it can describe the variations in wind speed to a certain degree. Therefore, d_1 and d_2 in equation (3) can be assumed to be invariant during a day period. When d_1 and d_2 are given, H at any time in a day can be calculated using equation (3) with known T_s and T_a. It should be noted that equation (3) is derived from the study of *Blümel* [1998] for H parameterization for unstable cases, but it will be used to estimate H over a day. Atmospheric stratification at night is generally stable, i.e., $T_{aero} - T_a < 0$; H is consequently negative during nighttime. Due to the amplification of $(T_s - T_a)^2$, even though $T_s - T_a < 0$, it is possible that H becomes a positive value based on equation (3). Therefore, for the estimation of H under the stable situation ($T_s - T_a < 0$ in this study) during a day, the right-second term in equation (3), i.e., $d_2[T_s - T_a]^2$, is neglected. Parameters d_1 and d_2 essentially depend on atmospheric and surface characteristics, e.g., the study of *Carlson and Buffum* [1989] concluded that the heat conductance is highly sensitive to wind speed, roughness, and vegetation amount. Therefore, d_1 and d_2 in the H parameterization of equation (3) vary with surface characteristics even for identical atmospheric condition.

2.2. Parameterization for Latent Heat Flux (LE)

In the *Raffy and Becker* [1985] study, H and LE were, respectively, parameterized as

$$H = \chi[F(T_s - T_a)] \tag{4}$$

$$LE = \chi M_s[FP_s(T_s)/\gamma] - \chi M_a e_a[FP_s(T_a)/\gamma] \tag{5}$$

where χ is the inverse of the resistance at neutrality for a wind velocity of 1 m/s (–); F in W/(m^2·K) is a universal function accounting for atmospheric instability and is constituted by T_s, T_a, and u; M_s is a parameter related to surface relative humidity, vegetation cover, aerodynamic resistance, and canopy resistance (-); M_a is similar to M_s; $P_s(T)$ is the saturated vapor pressure at temperature T (hPa); e_a is the relative humidity of the air (-); and γ is the psychometric constant with a slight temperature dependence (hPa/K).

Combining equations (4) and (3) results in the following equation:

$$\chi F = d_1 + d_2(T_s - T_a) \tag{6}$$

Replacing χF in equation (5) with equation (6), and writing $P_s(T_a)$ with Taylor series expansion of the first order at T_s, equation (5) becomes

$$LE = c\underbrace{[P_s(T_s)]}_{f_1} + d\underbrace{\left[\frac{\partial P_s(T)}{\partial T}\bigg|_{T=T_s} \times (T_s - T_a)\right]}_{f_2} + e\underbrace{[P_s(T_s) \times (T_s - T_a)]}_{f_3} + f\underbrace{\left[\frac{\partial P_s(T)}{\partial T}\bigg|_{T=T_s} \times (T_s - T_a)^2\right]}_{f_4} \tag{7}$$

with $c \approx (M_s - M_a e_a)d_1/\gamma$; $d \approx M_a e_a d_1/\gamma$; $e \approx (M_s - M_a e_a)d_2/\gamma$; and $f \approx M_a e_a d_2/\gamma$.

$\frac{\partial P_s(T)}{\partial T}|_{T=T_s}$ is the derivative of the saturated vapor pressure $P_s(T)$ at the $T = T_s$ (hPa/K). In this study, Tetens formula is adopted to compute the saturated vapor pressure from the temperature [*Campbell and Norman*,

1998], i.e., $P_s(T)=6.11\times\exp\left(\frac{17.502\times T}{T+240.97}\right)$ (T is the Celsius temperature). Therefore, at $T=20^{\circ}$C (293.15 K), $P_s(T)=23.36$ hPa, and $\frac{\partial P_s(T)}{\partial T}|_{T=293.15\ \mathrm{K}}=1.45$ hPa /K. Functions f_1, f_2, f_3, and f_4 in equation (7) are related to T_s and T_a. An approximate linear relationship between functions f_2 and f_3 can be obtained from equation (7) for the change range of temperature. Although the relationship between functions f_2 and f_4 is nonlinear, it is assumed to be linear in this study because of generally positive values of T_s-T_a. It is inevitable that some errors will be produced when T_s-T_a is small, but from trial analysis, the error is not more than 10 W/m^2 for *LE* estimate at the instantaneous time scale. Therefore, the assumption of linear relationship between functions f_2 and f_4 might be suggested. Because c, d, e, and f in equation (7) are nearly invariant over a day period according to the assumption of *Raffy and Becker* [1985], *LE* is finally parameterized as

$$LE=d_3[P_s(T_s)]+d_4\left[\frac{\partial P_s(T)}{\partial T}\bigg|_{T=T_s}\times(T_s-T_a)\right]+d_5 \tag{8}$$

where d_3 and d_4 are in W/(m^2·hPa) and can be considered as the heat conductance for vapor transfer; d_5 is in W/m^2 and is taken as a corrected term for *LE* estimates, which is a negative value by trial analysis. Similar to d_1 and d_2, parameters d_3, d_4, and d_5 in equation (8) are also invariant over a day period and vary with different days.

2.3. Parameterization for Soil Heat Flux (G)

In the study of *Bhumralkar* [1975], the soil temperature profile was solved from the heat conductivity equation by the expression of the sine function for T_s. As a result, G at depth x (m) and time t was given by

$$G(x,t)=(\omega c_s\lambda/2)^{1/2}\left[\omega^{-1}\frac{\partial T_s(x,t)}{\partial t}+T_s(x,t)-\overline{T}\right] \tag{9}$$

where ω is the frequency of oscillation (s^{-1}); c_s is the volumetric heat capacity of soil (J/(m^3·K)); λ is the soil thermal conductivity (J/(m·K·s)); $T_s(x, t)$ is the soil temperature at depth x and time t (K); $\frac{\partial T_s(x,t)}{\partial t}$ represents the change rate of the soil temperature (K/s); and $\overline{T}$ is the daily average temperature of the soil (K), which is assumed to be the same at all depths. Provided that there is no large change in ω, c_s, and λ in a day period, G at the surface is parameterized as

$$G(t)=d_6\left[\frac{\partial T_s(t)}{\partial t}\right]+d_7[(T_s(t)-\overline{T}_s)] \tag{10}$$

where d_6 ((W·s)/(m^2·K)) and d_7 (W/(m^2·K)) are assumed to be invariant over a day period. In equation (9), T_s represents the soil temperature, but in the new parameterization scheme shown in equation (10), T_s is taken as the surface radiative temperature that can be easily measured by remote sensing. When the surface is covered by vegetation, T_s is a mixed temperature for soil and vegetation. Therefore, d_6 and d_7 are not only related to soil properties but also depend on vegetation characteristics. All uncertainties in surface characteristics are encapsulated into d_6 and d_7. In this study, $T_s(t)$ is given by the Fourier expansion with order three from the measured T_s, so the integral of $\frac{\partial T_s(t)}{\partial t}$ and $T_s(t)-\overline{T}_s$ during a whole day is equal to 0. As a result, the daily G is 0 in the new parameterization scheme, which satisfies the assumption of negligible G at the daily time scale.

2.4. Estimation of H, LE, and G Based on Energy Balance

For estimating H, *LE*, and G by equations (3), (8), and (10), the key is to accurately solve for the constant parameters for a day period. The equation of surface energy balance in the vertical direction can be expressed by

$$R_n=H+LE+G \tag{11}$$

where R_n is the surface net radiation (W/m^2).

Combining equations (3), (8), and (10), R_n is written as

$$R_n(t)=\sum_{k=1}^{q} d_k \varphi_k(T_s, T_a, t) \tag{12}$$

where d_k are unknown constants; q is the number of unknown constants and is equal to 7 in this study; $\phi_k(T_s, T_a, t)$ ($k = 1, 2, 3, 4, 6, 7$) are the functions related to T_s and T_a within brackets in equations (3), (8), and (10), and ϕ_k ($k = 5$) is a unit vector, i.e., $\varphi_k(T_s, T_a, t)=\left\{(T_s-T_a), (T_s-T_a)^2, P_s(T_s), \frac{\partial P_s(T)}{\partial T}\Big|_{T=T_s} \times (T_s-T_a), 1, \frac{\partial T_s(t)}{\partial t}, (T_s(t)-\overline{T}_s)\right\}$. The flux minimization technique can be used to solve d_k when R_n is measured or obtained from remotely sensed data. This method is to solve the optimal parameters d_k to make the root mean square difference between R_n calculated by equation (12) and known R_n minimum. Therefore, the solutions of d_k are reduced to a linear system, i.e.,

$$\mathrm{A}\vec{d}=\vec{\mathrm{b}} \tag{13}$$

in which $\mathrm{A}_{ij}=\varphi_i(T_s, T_a, t_j), 1 \le i \le q, 1 \le j \le n$, and

$$\vec{\mathrm{b}}_j=R_n(t_j)$$

where n is the number of measurement. Taking the physical meaning of parameters d_k into consideration, the least-squares method with constraints is chosen to solve for d_k. In this study, the lsqlin function in MATLAB software is utilized to solve the constrained linear least-squares problems of equation (13), and the equation of lsqlin function is

$$\min \frac{1}{2}\left\|\mathrm{A}\vec{d}-\vec{\mathrm{b}}\right\|_2^2 \; such \;\; that \;\; \begin{cases} d_k(k=1,2,3,4,6,7) > 0 \\ d_k(k=5) < 0 \end{cases} \tag{14}$$

Details about lsqlin function can be referenced to the help file of MATLAB software. For input data of equation (14), because there are total seven unknown variables that need to be solved in equations (3), (8), and (10), n ($n \ge 7$) sets of known values of T_s, T_a, and R_n for a day period are required as inputs. n sets of known values of T_s, T_a, and R_n should be able to reflect changing trend in T_s, T_a, and R_n over a day period. In addition, the unstable atmospheric situation during daytime is also required. This is because the parameterization for H is derived using the Richardson number in unstable stratification.

After d_k is determined, H, LE, and G at any time during a day can be estimated by equations (3), (8), and (10) in combination with known T_s and T_a, and then the daily H, LE, and G can be calculated by averaging instantaneous H, LE, and G during a day. The complete procedure for H, LE, and G estimates is shown in Figure 1.

3. Data

The Yucheng station (36.8291°N, 116.5703°E), located southwest of Yucheng County, Shandong Province in North China, is a part of the Chinese terrestrial ecosystem flux network and aims at measuring the exchange of carbon dioxide, water vapor, and heat between the land and the atmosphere. The climate is a subhumid and the monsoon climate with a mean annual temperature and precipitation of 13.1°C and 528 mm, respectively. Winter wheat and summer maize are generally cultivated by rotation at this site. The stages of wheat and corn growth in 2010 are displayed in Figure 2. The leaf area index (LAI) measured by a portable leaf area meter (LI-3000) and the crop height are also shown in Figure 2.

The measurements from the Yucheng station in year 2010, including meteorological variables, radiation, and fluxes, were collected to evaluate the simplified parameterization schemes and the method of estimating surface fluxes based on energy balance. Meteorological variables, including air temperature, wind speed, relative humidity, and atmospheric pressure, were measured at the height of 2.93 m during the period of wheat growth and at 4.2 m during the period of corn growth. H and LE were measured by an

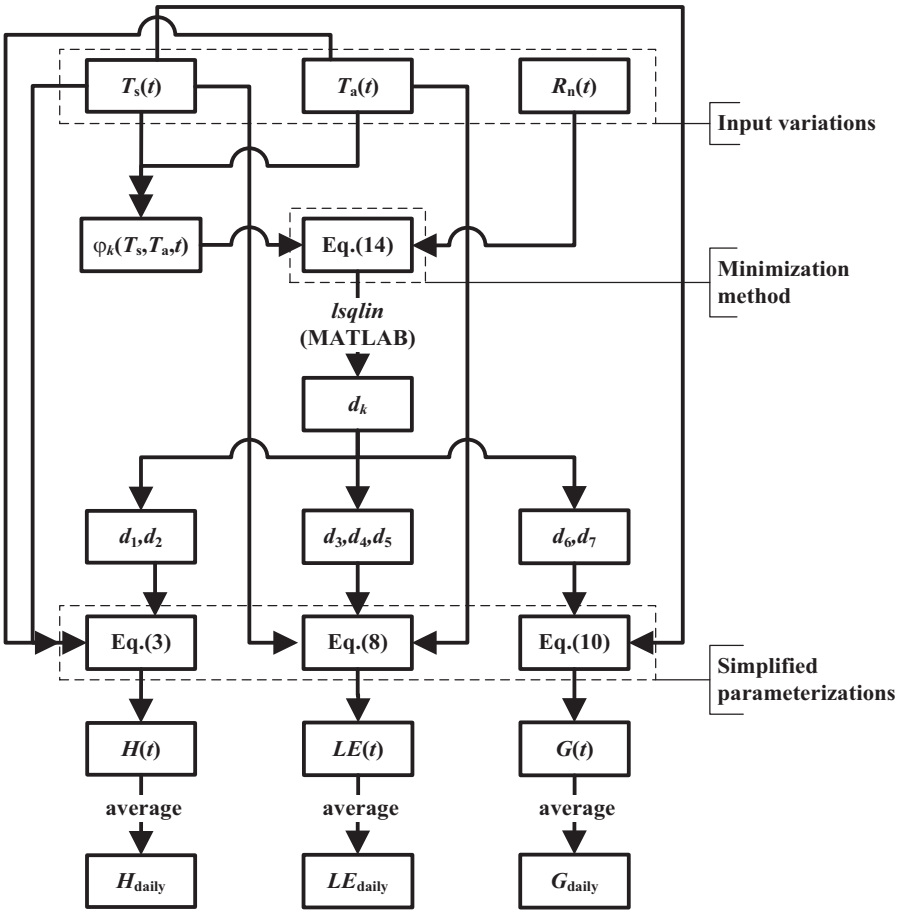

Figure 1. Flow chart of surface energy fluxes estimates.

eddy covariance (EC) system consisting of an open-path CO_2/H_2O gas analyzer and a 3-D sonic anemometer/thermometer. The height of the EC was 2.7 m during the period of wheat growth and was elevated to 3.75 m during the period of corn growth. Four-component radiation, i.e., the downwelling and upwelling shortwave radiation, and the downwelling and upwelling longwave radiation, was acquired from a CNR-1 installed at a height of 3.98 m. G was estimated from a single HFP-01 soil heat flux plate at 2 cm soil depth without considering heat transfer for the 2 cm storage layer above the plate. All data are recorded as a 30 min average, so there are 48 records in a day for each variable. T_a and R_n observations were used to drive parameterization schemes, and the measured H, LE, and G are used to validate the results. T_s is not directly measured but rather is calculated by the following formula:

$$T_s=((L_u-(1-\varepsilon)L_d)/\sigma\varepsilon)^{1/4} \tag{15}$$

where L_u and L_d are the upwelling and downwelling longwave radiation (W/m^2), respectively; ε is the surface emissivity and is assumed to be 0.98 in this study [*Li et al.*, 2013b]; and σ is the Stefan-Boltzmann constant (5.67×10^{-8} W/m^2·K^4).

To ensure the atmospheric stratification is unstable during the daytime, data that $T_s - T_a$ in a day are all less than 1 K were removed from the analysis. The threshold value of 1 K is to better exclude those transition states due to the difference of T_s and T_{aero}. Based on the incoming solar radiation and available measured data, 40 cloud-free days at the Yucheng station in 2010 were finally selected. The selected days are marked by black filled circles in Figure 2. Energy balance nonclosure is the primary source of error for EC measurements [*Twine et al.*, 2000]. Figure 3 compares $R_n - G$ with $H + LE$ from EC measurements at the Yucheng station for the selected days. At the instantaneous time scale, the root mean square error (RMSE) of measured

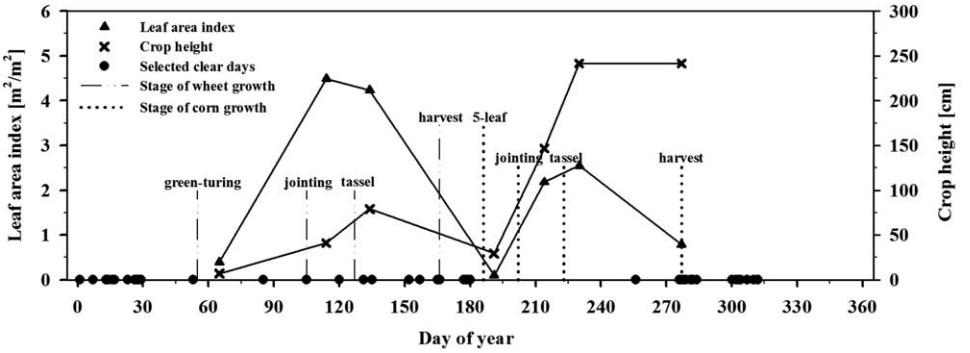

Figure 2. Surface characteristics of the Yucheng station in year 2010.

$H + LE$ with respect to measured $R_n - G$ is 44.8 W/m^2 with a coefficient of determination (R^2) of 0.938, and at the daily scale, the RMSE is 19.6 W/m^2 with an R^2 of 0.945. The linear least-squares fit of $H + LE$ to $R_n - G$ shows a slope of 0.785 and an intercept of 21.7 W/m^2 at the instantaneous scale, and a slope of 0.741 and an intercept of 24.2 W/m^2 at the daily scale. From Figure 3, it can be observed that energy balance nonclosure primarily occurs in the high end of $R_n - G$, whereas measured $H + LE$ is larger than $R_n - G$ in the low end. The mismatch of the footprints of turbulent (H and LE) and nonturbulent (R_n and G) fluxes, different observation scales among instruments, and the errors in measurements may cause the energy balance nonclosure.

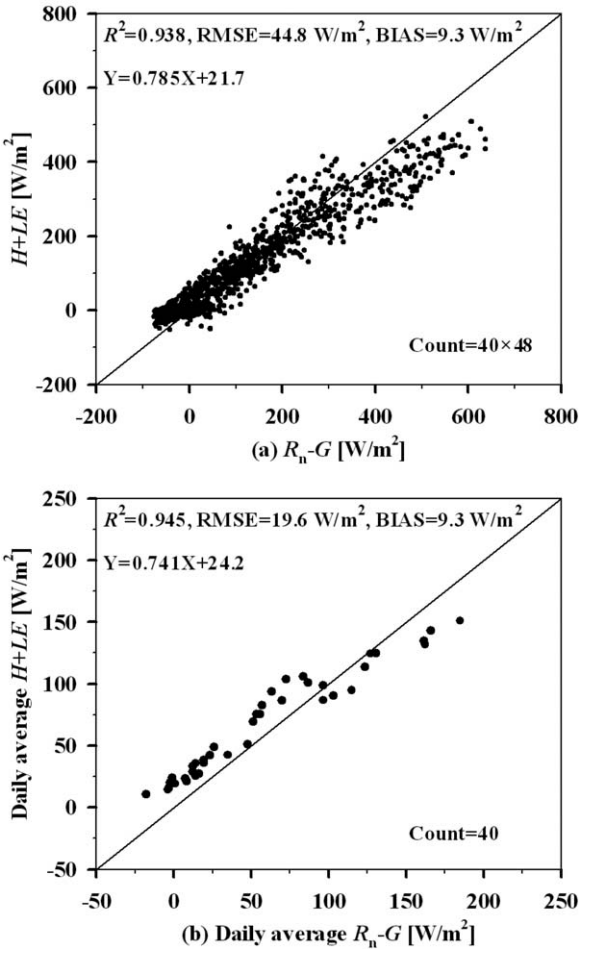

Figure 3. Comparison between $R_n - G$ and $H + LE$ from EC measurements at the Yucheng station for the selected 40 clear days with (a) a 30 min average and (b) daily average.

4. Results and Discussion

The simplified parameterizations for H, LE, and G (equations (3), (8), and (10)) and the estimation of surface fluxes based on the energy balance (equation (14)) are the two important components of the method shown in section 2. The ability of the simplified schemes of equations (3), (8), and (10) to depict variations in H, LE, and G over a day will be examined using the measured H, LE, and G at the Yucheng station in section 4.1. For H, LE, and G estimation, the critical process is to obtain those constants ($d_{1\text{-}7}$) in the simplified parameterizations, which can be solved by equation (14) with known T_s, T_a, and R_n as inputs. Input data used in this section are from the Yucheng station measurements. The results will be discussed in section 4.2.

4.1. Performance of Simplified Parameterizations

The principal procedure for surface energy fluxes estimation is first to simplify H, LE, and G as

some parameters that are invariant over a day and some functions that depend on T_s and T_a. Although the assumption of constant parameters can be met theoretically, they need to be further demonstrated by actual *H*, *LE*, and *G*. With known *H*, *LE*, and *G* from the Yucheng station measurements, those parameters assumed to be invariant over a day can be solved by equations (3), (8), and (10) using the least-squares method with constraints. The solutions are regarded as the "true values" of parameters d_k, which are shown in Figure 4 (see filled triangle symbols). It can be found that parameters d_{1-5}, corresponding to the heat conductance for sensible and latent heat transfer, are generally related to LAI, whereas parameters d_{6-7} do not strongly change with LAI. However, these relationships between parameters d_k and LAI are not unique because parameters d_k essentially vary with atmospheric and surface conditions.

H, *LE*, and *G* calculated by the least-squares solutions of equations (3), (8), and (10) are taken as the parameterized results. The parameterized results for selected 40 clear days are plotted in Figure 5. From Figure 5a, it can be obtained that equation (3) underestimates *H* by 6.6 W/m^2 with an R^2 of 0.921 and an RMSE of 19.7 W/m^2. It seems that equation (3) underestimates *H* when the measured *H* varies from 0 to 100 W/m^2. This may be attributed to the difference between T_{aero} and T_s. It is the T_{aero} which determines the loss of *H* from a surface. Because T_{aero} is not easily measured in reality, the atmospheric status is judged by $T_s - T_a$ in this

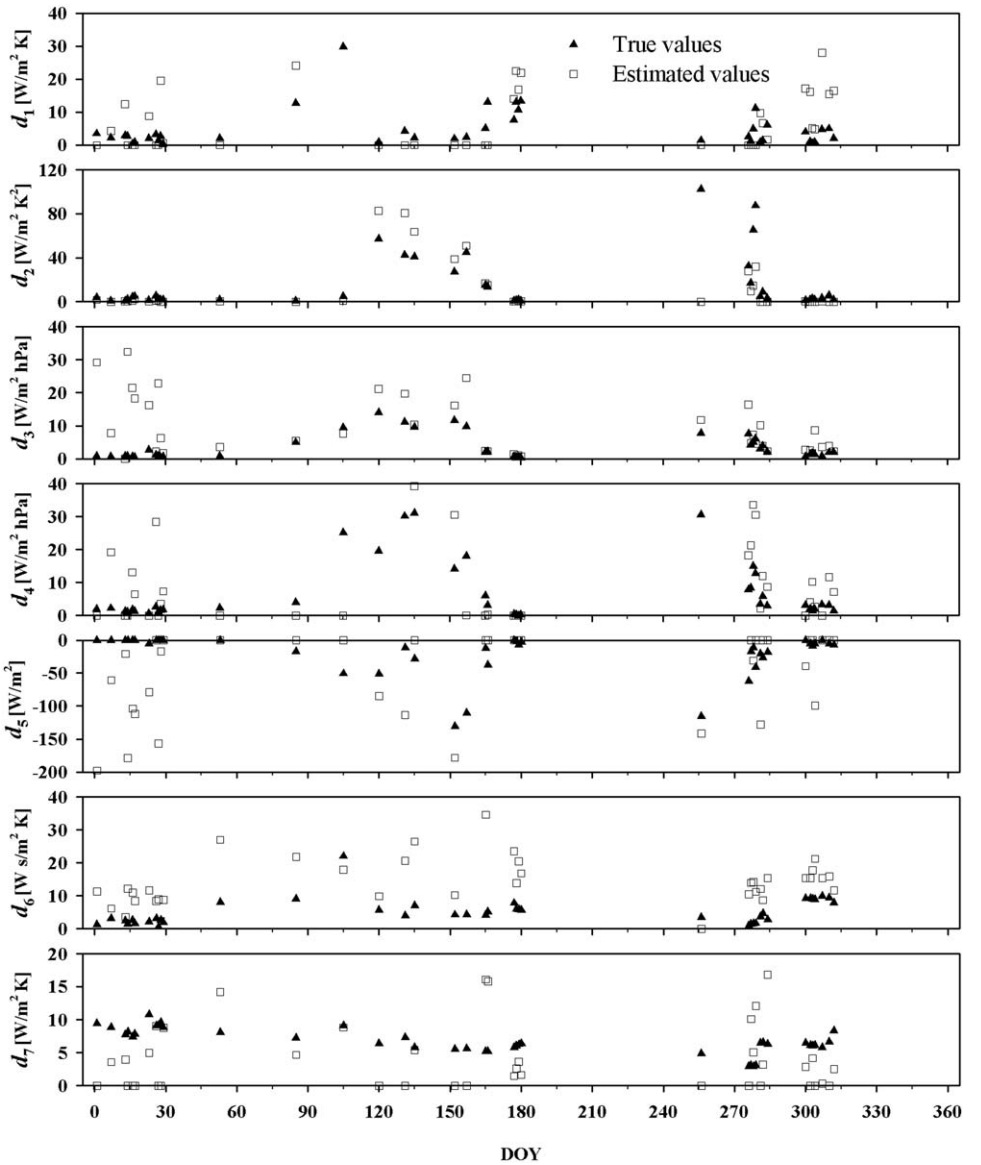

Figure 4. Values of parameters d_k for 40 selected days from the Yucheng station.

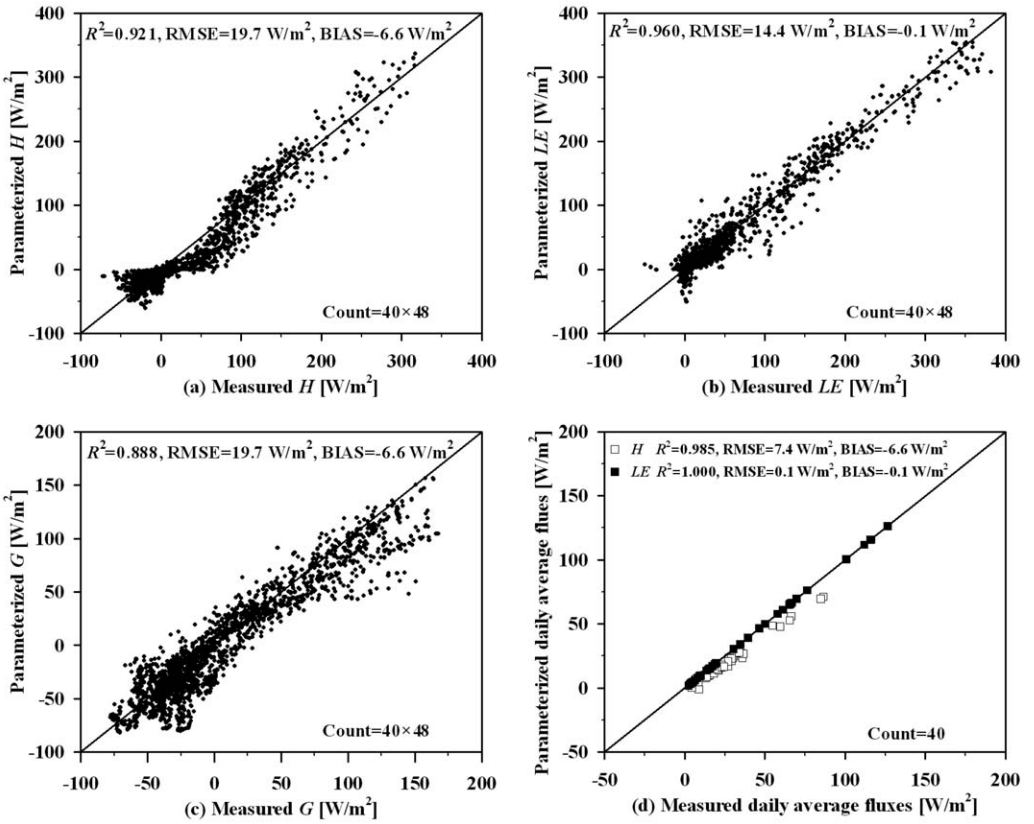

Figure 5. Comparisons of parameterized (a) *H*, (b) *LE*, (c) *G*, and (d) daily average fluxes from equations (3), (8), and (10) with corresponding ground-based measurements.

study. $T_s - T_a < 0$ (stable atmospheric condition) corresponds to the negative *H* according equation (3), but the actual *H* which depends on $T_{aero} - T_a$ may be not less than 0. In addition, the inconsistent observation scales on *H*, T_s, and T_a and the errors in measurements also lead to the parameterized results differing from the measured values. In reality, it seems extremely difficult to evaluate the atmospheric status by a single criterion. Therefore, at some transition status, a larger discrepancy is observed. Equation (8) can well describe the *LE* from EC measurements with an R^2 of 0.960 and an RMSE of 14.4 W/m^2. Although there are some uncertainties in the measurement of *G* from the soil heat flux plate located 2 cm below the surface, the measured *G* can be well reproduced by equation (10) with an R^2 of 0.888 and an RMSE of 19.7 W/m^2 (see Figure 5c). The error in the *G* parameterization also originates from the implicit assumption of equation (10), i.e., daily *G* is equal to 0. However, actual daily *G* may not seamlessly satisfy this assumption. T_s and its change rate with time are two main inputs in the *G* parameterization. In this study, the change rate of T_s with time is obtained by the Fourier expansion of T_s. Errors of T_s from the Fourier expansion with order three can, therefore, influence the accuracy of *G*. In addition, T_s is not directly measured but is calculated by equation (15). The assumption of surface emissivity with 0.98 in equation (15) also brings some errors.

At the daily scale (see Figure 5d), *H* and *LE* from the simplified parameterizations show a higher accuracy than that at the instantaneous time scale, with an R^2 of 0.985 and an RMSE of 7.4 W/m^2 for *H* and an R^2 of 1.0 and an RMSE of 0.1 W/m^2 for *LE*. The daily average *LE* from equation (8) is nearly equal to those measured values. *G* from equation (10) at the daily scale is equal to 0, so it is not displayed in Figure 5d. All results shown in Figure 5 can demonstrate that surface energy fluxes *H*, *LE*, and *G* can be expressed by some invariant parameters over a day period and the functions related to T_a and T_s with the RMSE of ~20 W/m^2.

4.2. Evaluation of *H*, *LE*, and *G* Estimates

With measured R_n, T_a, and T_s at the Yucheng station, constant parameters d_k for a given day are solved by equation (14) and d_k values are then used to estimate *H*, *LE*, and *G* using equations (3), (8), and (10). The results for *H*, *LE*, and *G* estimates at the instantaneous time scale are displayed in Figure 6. The RMSE for the

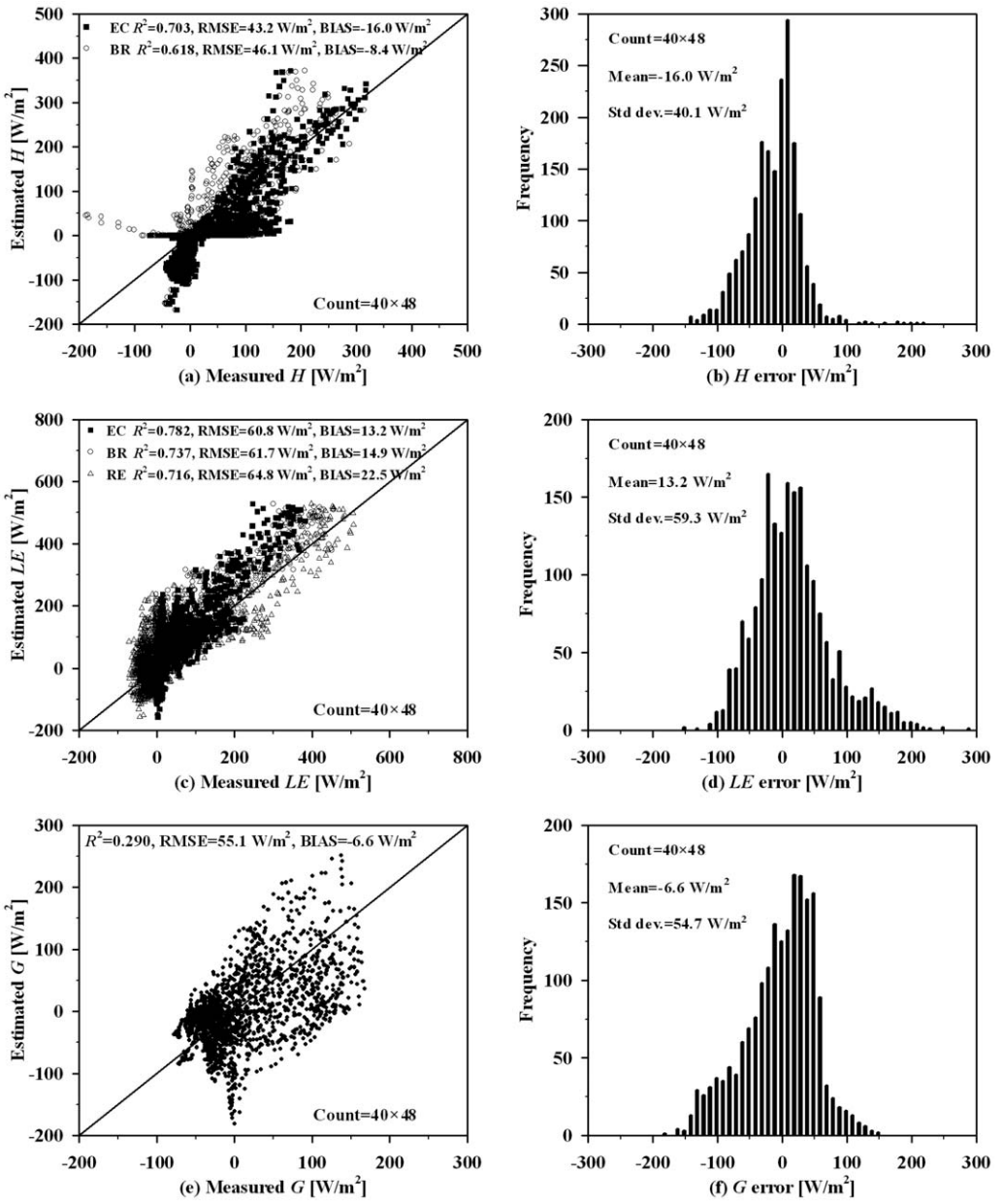

Figure 6. Comparisons of (a) *H*, (c) *LE*, and (e) *G* at the instantaneous time scale estimated by equation (14) with measured values, and error distributions for (b) *H*, (d) *LE*, and (f) *G* estimates.

H estimates is 43.2 W/m^2 with an R^2 of 0.703 (see black squares in Figure 6a). The error distribution histogram in Figure 6b shows the majority of the errors (>90%) for *H* estimates vary from −70 to 70 W/m^2. For *LE* estimates from equation (14), the estimated values are closely related to actual measured values with an R^2 of 0.782 and the RMSE is 60.8 W/m^2 (see black squares in Figure 6c). The histogram of error distribution shows that the majority of errors (>90%) for *LE* estimates range from −100 to 100 W/m^2 (see Figure 6d). Different from existing ET models, it is unnecessary that *G* is given beforehand. *G* at any time in a day period can be estimated by equation (10) with the constant parameters obtained from equation (14), but with an assumption of daily *G* equal to 0. The results in Figure 6e show that the RMSE for *G* estimates at the instantaneous scale are 55.1 W/m^2 with an R^2 of 0.290, and the majority of errors (>90%) vary from −90 to 90 W/m^2 (see Figure 6f).

Energy balance nonclosure in EC-based measurements is a source of error leading to the inconsistency between estimated and measured values. Two correction methods, i.e., the residual energy (RE) method

and the Bowen ratio (BR) method, are often used to correct the EC-measured *LE* [*Twine et al*., 2000]. The RE method assumes that the EC-measured *H* is accurate, and all imbalance energy is assigned to *LE*, that is, the *LE* corrected by the RE method is equal to the value of surface available energy minus the EC-measured *H*. The BR method assumes that energy balance nonclosure is caused not only by EC-measured *LE* but also by EC-measured *H*, and the imbalance energy is partitioned into *H* and *LE* according to the Bowen ratio. Because of unstable Bowen ratio values during nighttime, in this study, the daily average Bowen ratio is assumed to be invariant after the EC-measured *H* and *LE* are corrected. When *H* and *LE* at the instantaneous time scale estimated from equation (14) are compared with the values corrected by BR method (see circle symbols in Figures 6a and 6c), the results do not improve. This may indicate that the BR method is not appropriate for the correction of EC-measured *H* and *LE* at the Yucheng station. After the EC-measured *LE* is corrected by the RE method, because energy balance nonclosure primarily occurs at high $R_n - G$, the *LE* estimates are closer to the corrected measurements when the *LE* magnitude is large, whereas the results worsen in low end because measured $H + LE$ is greater than $R_n - G$ (see triangle symbols in Figure 6c). This may conclude that it is not rather reasonable to correct EC-measured low *LE* by the RE method.

The results for *H* and *LE* estimates at the daily scale are displayed in Figure 7. The accuracy at the daily scale is generally better than that at the instantaneous time scale shown in Figure 6. Daily average *H* estimates is closer to the BR-corrected measurements with an R^2 of 0.666 and an RMSE of 16.9 W/m^2. For daily average *LE* estimates, the discrepancy between the estimated and the measured results is reduced to 23.2 W/m^2 (0.8 mm/d or relative RMSE of 61%), and R^2 is increased to 0.860. The high relative RMSE of 61% occurs because more of the selected data have a low ET. Similar to the results shown in Figure 6c, the estimated daily average *LE* is also closer to the corrected measurements when the *LE* magnitude is large. In addition, measurement error, mismatch of footprints between radiation and fluxes, and other uncertainties can also cause the discrepancy between the estimated values and measurements.

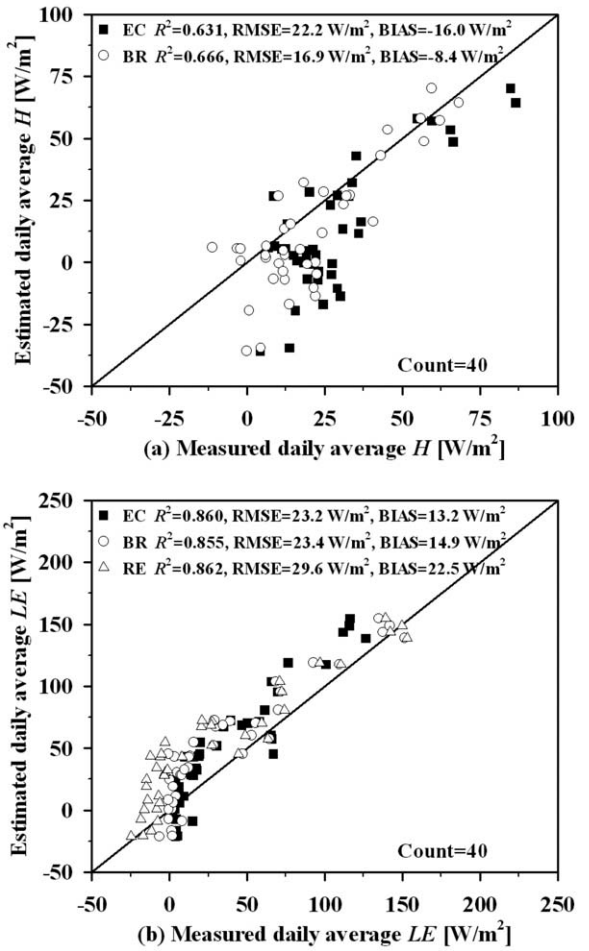

Figure 7. Comparisons of the estimated daily average (a) *H* and (b) *LE* with the EC-based measurements and corrected values.

Because *LE* is more meaningful in a range of hydrologic, ecological, and climatic studies and applications, the accuracy of *LE* estimates obtained here of ~60 W/m^2 at the instantaneous time scale and ~20 W/m^2 (~0.8 mm/d) at the daily scale is encouraging compared with similar studies from the current ET model. For example, *Tang et al*. [2011] found that the RMSE were ~45, 55, and 110 W/m^2 when the two-source energy balance model [*Norman et al*., 1995], the surface energy balance system (SEBS) model [*Su*, 2002], and the triangle model were used to estimate *LE* at the Yucheng station, respectively. The accuracy for *LE* estimates from the spatial variability models, including triangle, surface energy balance algorithm

for land (SEBAL) [*Bastiaanssen et al*., 1998], and mapping ET at high resolution with internalized calibration (METRIC) [*Allen et al*., 2007] models, is ~35–80 W/m^2 [*Long and Singh*, 2013]. For daily ET estimates, the accuracy from the upscaling EF schemes is about 0.2–1.4 mm/d [*Colaizzi et al*., 2006; *Sobrino et al*., 2007; *Tang et al*., 2013b].

The results estimated from equation (14) shown in Figures 6 and 7 are not consistent with the parameterized results shown in Figure 5. This is essentially because the parameters d_k obtained by the least-squares method with constraints are not equal to those "true values" (see open squares in Figure 4). Apart from the uncertainties in measurements as discussed above, another main reason for the inconsistency is that the errors in input variables cause instability of the solution to the linear system of equation (13). This may be also explained by the fact that only two known variables T_s and T_a are used to construct the linear system with seven unknown parameters. Intrinsic interactions among those known functions depending on T_s and T_a can result in the interdependency among the solutions to equation (13). As a result, as shown in Figure 7, for daily average H and LE estimates, H is underestimated and LE is overestimated. Because of the errors in input variables, the solution to equation (13) is essentially converted to solving an ill-posed problem. It is, however, difficult to obtain the true solutions due to the nature of the ill-posed problem [*Beven and Freer*, 2001], and an approximate solution is often given. From Figure 4, it can be observed that most of d_k estimated by the least-squares method with constraints are distributed around their "true values" (see Figure 4), but there are some obvious deviating values which cause the errors in the estimated surface energy fluxes.

The least-squares method with constraints, i.e., equation (14), is a simple scheme to obtain an approximate solution of the ill-posed problem. The regulation method and particle swarm optimization are often used to solve this problem [*Kennedy and Eberhart*, 1995; *Tikhonov and Arsenin*, 1977], but these methods are not used in this study because of sophisticated mathematic theory. *Sun et al*. [2011, 2012] put forward a new stationarity-based method to estimate the parameters of a land surface water and energy balance model and then used the estimated parameters to obtain surface energy fluxes without the calibration of flux observation, which are similar to our method. However, compared with their method, our method is simpler, the parameterizations for surface energy fluxes are simplified, and only surface temperature, air temperature, and net radiation are required as inputs. The stationarity-based scheme can be referenced to further improve the solution of constant parameters in our future study. In addition, to classify the values of parameter d_k according to different atmospheric and surface characteristics, and then to constrain equation (14) is also another way to obtain more accurate approximate solution, but the methodology for selecting the proper categories for d_k should be further investigated.

5. Summary and Conclusion

This study develops a new method of estimating surface H, LE, and G from continuous T_s, T_a, and R_n observations over a day without calculating various surface resistances. The parameterization schemes of H, LE, and G are first simplified as equations (3), (8), and (10) consisting of unknown constant parameters that remain fairly invariant throughout a day and known functions related to T_s and T_a. On the basis of surface energy balance, with known R_n over a day, unknown constants can be solved by equation (14) using a least-squares method with constraints. The results from ground-based measurements indicate that the simplified parameterization schemes of equations (3), (8), and (10) can well reproduce H, LE, and G at the instantaneous time scale with an RMSE of ~20 W/m^2, and the accuracy at the daily scale is generally higher than that at the instantaneous time scale. When surface energy fluxes are simultaneously estimated by the solution of equation (14) with known R_n, T_s, and T_a from the Yucheng station measurements, the RMSE for H, LE, and G estimates is ~60 W/m^2 at the instantaneous time scale, and ~20 W/m^2 at the daily scale. Although there are various uncertainties in the measurements, most of the results estimated by equation (14) are encouraging.

The main advantages of the method developed in this study include: (1) fewer inputs, only T_s, T_a, and R_n are required; (2) it does not need to calculate various resistances depending on surface and atmospheric characteristics; and (3) H, LE, and G can be estimated simultaneously. Requirements of the developed method should be clear before its implementation:

(1) Continuous values for T_s, T_a, and R_n during a day are required. It should be clarified that continuous values are not the values at every time during a day but are multiple observations (at least seven) that can

reflect changing trends in T_s, T_a, and R_n in a day. This requirement would make this method not applicable to polar satellites because of the limited observations in a day. However, the strength of this method would be manifested using geostationary meteorological satellites. Under clear-sky conditions, geostationary meteorological satellites with thermal infrared sensors, e.g., the Spinning Enhanced Visible and Infrared Imager onboard the Meteosat Second Generation (MSG-SEVIR), Geostationary Operational Environmental Satellites (GOES 8), and Chinese geostationary FengYun meteorological satellite (FY-2C), can provide multiple T_s observation in a day with a 15 or 30 min internal, and the RMSE is about 1–2 K [*Jiang and Li*, 2008; *Sun et al*., 2004; *Tang et al*., 2008]. Diurnal T_a can be estimated from MSG-SEVIRI data with an RMSE of ~3 K [*Stisen et al*., 2007], and the overall bias uncertainty in GOES satellite-retrieved R_n approximated 7.5% [*Gu et al*., 1999]. These studies provide data sources for the developed method. Note that it is inevitable that the surface parameters from geostationary satellites are subject to the very coarse spatial resolution. Because of the heterogeneity of land surface, the coarse spatial resolution may bring a lot of uncertainties in the retrieved surface parameters from remote sensing. However, use of continuous inputs in new developed method can obviate the calculation of various resistances for surface energy estimates. Furthermore, use of temporal information can make surface flux estimates insensitive to errors in remotely sensed variables at the instantaneous time scale. Applications of the method using remotely sensed data will be given in future studies.

(2) Unstable atmospheric conditions during daytime are required for the parameterization scheme of H, which could be satisfied in most cases in reality. For the stable atmospheric stratification during daytime, a new parameterization for H or some constraints may be required, but this study does not address this issue.

(3) Although the results from equation (14) in section 4.2 are generally acceptable, there is still a gap between the estimates from equation (14) and the parameterized results from equations (3), (8), and (10) due to the instability of linear system of equation (13). Solving ill-posed problem is a hot spot of research in many fields, such as remote sensing, signal processing, geographical inversions, and industrial control. Advances in solving ill-posed problems in these fields should be helpful in deriving more accurate constant parameters over a day period in the future. In addition, incorporating a prior knowledge of constant parameters into the solving processes also warrants further study.

Acknowledgments

We greatly thank Di Long from the Bureau of Economic Geology, Jackson School of Geosciences, The University of Texas at Austin, who provided many constructive comments for improving this study and help with polishing the language of this manuscript. We also thank the Associate Editor and two reviewers for providing excellent suggestions and comments. This work was partly supported by the National Natural Science Foundation of China under grants 41201366 and 41101332 and by the China Postdoctoral Science Foundation funded project under grant 07Z7602MZ1. Jing Lu is financially supported by China Scholarship Council for her stay in ICube, Strasbourg, France.

References

Abdellaoui, A., F. Becker, and E. Olory-Hechinger (1986), Use of meteosat for mapping thermal inertia and evapotranspiration over a limited region of Mali, *J. Appl. Meteorol.*, *25*, 1489–1506, doi:10.1175/1520-0450(1986)025<1489:UOMFMT>2.0.CO;2.

Allen, R. G., M. Tasumi, and R. Trezza (2007), Satellite-based energy balance for mapping evapotranspiration with internalized calibration (METRIC)—Model, *J. Irrig. Drain. Eng.*, *133*(4), 380–394, doi:10.1061/(ASCE)0733-9437(2007)133:4(380).

Anderson, M. C., J. M. Norman, G. R. Diak, W. P. Kustas, and J. R. Mecikalski (1997), A two-source time-integrated model for estimating surface fluxes using thermal infrared remote sensing, *Remote Sens. Environ.*, *60*(2), 195–216, doi:10.1016/s0034-4257(96)00215-5.

Bastiaanssen, W. G. M., M. Menenti, R. A. Feddes, and A. A. M. Holtslag (1998), A remote sensing surface energy balance algorithm for land (SEBAL). 1. Formulation, *J. Hydrol.*, *212*, 198–212, doi:10.1016/S0022-1694(98)00253-4.

Beven, K., and J. Freer (2001), Equifinality, data assimilation, and uncertainty estimation in mechanistic modelling of complex environmental systems using the GLUE methodology, *J. Hydrol.*, *249*(1), 11–29, doi:10.1016/S0022-1694(01)00421-8.

Bhumralkar, C. M. (1975), Numerical experiments on the computation of ground surface temperature in an atmospheric general circulation model, *J. Appl. Meteorol.*, *14*(7), 1246–1258, doi:10.1175/1520-0450(1975)014<1246:NEOTCO>2.0.CO;2.

Blümel, K. (1998), Estimation of sensible heat flux from surface temperature wave and one-time-of-day air temperature observation, *Boundary Layer Meteorol.*, *86*(2), 193–232, doi:10.1023/A:1000659320836.

Boni, G., D. Entekhabi, and F. Castelli (2001), Land data assimilation with satellite measurements for the estimation of surface energy balance components and surface control on evaporation, *Water Resour. Res.*, *37*(6), 1713–1722, doi:10.1029/2001WR900020.

Brutsaert, W. (1982), *Evaporation into the Atmosphere: Theory, History, and Applications*, D. Reidel, Dordrecht, Netherlands.

Campbell, G. S., and J. M. Norman (1998), *Introduction to Environmental Biophysics*, Springer, New York.

Caparrini, F., F. Castelli, and D. Entekhabi (2003), Mapping of land-atmosphere heat fluxes and surface parameters with remote sensing data, *Boundary Layer Meteorol.*, *107*(3), 605–633, doi:10.1023/A:1022821718791.

Carlson, T. N., and M. J. Buffum (1989), On estimating total daily evapotranspiration from remote surface temperature measurements, *Remote Sens. Environ.*, *29*(2), 197–207, doi:10.1016/0034-4257(89)90027-8.

Colaizzi, P. D., S. R. Evett, T. A. Howell, and J. A. Tolk (2006), Comparison of five models to scale daily evapotranspiration from one-time-of-day measurements, *Trans. ASABE*, *49*(5), 1409–1417.

Courault, D., B. Seguin, and A. Olioso (2005), Review on estimation of evapotranspiration from remote sensing data: From empirical to numerical modeling approaches, *Irrig. Drain. Syst.*, *19*(3–4), 223–249, doi:10.1007/s10795-005-5186-0.

Farahani, H. J., T. A. Howell, W. J. Shuttleworth, and W. C. Bausch (2007), Evapotranspiration: Progress in measurement and modeling in agriculture, *Trans ASABE*, *50*(5), 1627–1638.

Gu, J., E. A. Smith, and J. D. Merritt (1999), Testing energy balance closure with GOES-retrieved net radiation and in situ measured eddy correlation fluxes in BOREAS, *J. Geophys. Res.*, *104*(D22), 27,881–27,827, 27,893, doi:10.1029/1999JD900390.

Jackson, R. D., R. J. Reginato, and S. B. Idso (1977), Wheat canopy temperature: A practical tool for evaluating water requirements, *Water Resour. Res.*, *13*(3), 651–656, doi:10.1029/WR013i003p00651.

Jiang, G. M., and Z.-L. Li (2008), Split-window algorithm for land surface temperature estimation from MSG1-SEVIRI data, *Int. J. Remote Sens.*, *29*(20), 6067–6074, doi:10.1080/01431160802235860.
Jiang, L., and S. Islam (1999), A methodology for estimation of surface evapotranspiration over large areas using remote sensing observations, *Geophys. Res. Lett.*, *26*(17), 2773–2776, doi:10.1029/1999gl006049.
Jung, M., et al. (2010), Recent decline in the global land evapotranspiration trend due to limited moisture supply, *Nature*, *467*(7318), 951–954, doi:10.1038/nature09396.
Kalma, J. D., T. R. McVicar, and M. F. McCabe (2008), Estimating land surface evaporation: A review of methods using remotely sensed surface temperature data, *Surv. Geophys.*, *29*(4–5), 421–469, doi:10.1007/s10712-008-9037-z.
Kennedy, J., and R. Eberhart (1995), Particle swarm optimization, in *Proceedings of the IEEE International Conference on Neural Networks*, vol. 4, edited by IEEE Neural Networks Council, pp. 1942–1948, doi:10.1109/ICNN.1995.488968.
Lathuillière, M. J., M. S. Johnson, and S. D. Donner (2012), Water use by terrestrial ecosystems: Temporal variability in rainforest and agricultural contributions to evapotranspiration in Mato Grosso, Brazil, *Environ. Res. Lett.*, *7*(2), 024024, doi:10.1088/1748-9326/7/2/024024.
Li, Z.-L., R. L. Tang, Z. M. Wan, Y. Y. Bi, C. H. Zhou, B. H. Tang, G. J. Yan, and X. Y. Zhang (2009), A review of current methodologies for regional evapotranspiration estimation from remotely sensed data, *Sensors*, *9*(5), 3801–3853, doi:10.3390/s90503801.
Li, Z.-L., B. H. Tang, H. Wu, H. Ren, G. Yan, and Z. Wan (2013a), Satellite-derived land surface temperature: Current status and perspectives, *Remote Sens. Environ.*, *131*, 14–37, doi:10.1016/j.rse.2012.12.008.
Li, Z.-L., H. Wu, N. Wang, S. Qiu, J. A. Sobrino, Z. M. Wan, B. H. Tang, and G. J. Yan (2013b), Land surface emissivity retrieval from satellite data, *Int. J. Remote Sens*, *34*(9–10), 3084–3127, doi:10.1080/01431161.2012.716540.
Long, D., and V. P. Singh (2012), A two-source trapezoid model for evapotranspiration (TTME) from satellite imagery, *Remote Sens. Environ.*, *121*(0), 370–388, doi:10.1016/j.rse.2012.02.015.
Long, D., and V. P. Singh (2013), Assessing the impact of end-member selection on the accuracy of satellite-based spatial variability models for actual evapotranspiration estimation, *Water Resour. Res.*, *49*(5), 2601–2618, doi:10.1002/wrcr.20208.
Long, D., V. P. Singh, and B. R. Scanlon (2012), Deriving theoretical boundaries to address scale dependencies of triangle models for evapotranspiration estimation, *J. Geophys. Res.*, *117*, D05113, doi:10.1029/2011jd017079.
Lu, J., R. L. Tang, H. J. Tang, and Z.-L. Li (2013), Derivation of daily evaporative fraction based on temporal variations in surface temperature, air temperature, and net radiation, *Remote Sens.*, *5*(10), 5369–5396, doi:10.3390/rs5105369.
McLaughlin, D., Y. H. Zhou, D. Entekhabi, and V. Chatdarong (2006), Computational issues for large-scale land surface data assimilation problems, *J. Hydrometeorol.*, *7*(3), 494–510, doi:10.1175/JHM493.1.
Moran, M. S., T. R. Clarke, Y. Inoue, and A. Vidal (1994), Estimating crop water deficit using the relation between surface-air temperature and spectral vegetation index, *Remote Sens. Environ.*, *49*(3), 246–263, doi:10.1016/0034-4257(94)90020-5.
Mu, Q. Z., M. S. Zhao, and S. W. Running (2011), Improvements to a MODIS global terrestrial evapotranspiration algorithm, *Remote Sens. Environ.*, *115*(8), 1781–1800, doi:10.1016/j.rse.2011.02.019.
Nagler, P. L., J. Cleverly, E. Glenn, D. Lampkin, A. Huete, and Z. M. Wan (2005), Predicting riparian evapotranspiration from MODIS vegetation indices and meteorological data, *Remote Sens. Environ.*, *94*(1), 17–30, doi:10.1016/j.rse.2004.08.009.
Norman, J. M., W. P. Kustas, and K. S. Humes (1995), Source approach for estimating soil and vegetation energy fluxes in observations of directional radiometric surface-temperature, *Agric. For. Meteorol.*, *77*(3–4), 263–293, doi:10.1016/0168-1923(95)02265-Y.
Raffy, M., and F. Becker (1985), An inverse problem occurring in remote-sensing in the thermal infrared bands and its solutions, *J. Geophys. Res.*, *90*(D3), 5809–5819, doi:10.1029/Jd090id03p05809.
Raffy, M., and F. Becker (1986), A stable iterative procedure to obtain soil surface parameters and fluxes from satellite data, *IEEE Trans. Geosci. Remote Sens.*, *24*(3), 327–332, doi:10.1109/Tgrs.1986.289560.
Seguin, B., and B. Itier (1983), Using midday surface temperature to estimate daily evaporation from satellite thermal IR data, *Int. J. Remote Sens.*, *4*(2), 371–383, doi:10.1080/01431168308948554.
Seneviratne, S. I., D. Luthi, M. Litschi, and C. Schar (2006), Land-atmosphere coupling and climate change in Europe, *Nature*, *443*(7108), 205–209, doi:10.1038/nature05095.
Sobrino, J. A., M. Gomez, J. C. Jimenez-Muoz, and A. Olioso (2007), Application of a simple algorithm to estimate daily evapotranspiration from NOAA-AVHRR images for the Iberian Peninsula, *Remote Sens. Environ.*, *110*(2), 139–148, doi:10.1016/j.rse.2007.02.017.
Stisen, S., I. Sandholt, A. Nørgaard, R. Fensholt, and L. Eklundh (2007), Estimation of diurnal air temperature using MSG SEVIRI data in West Africa, *Remote Sens. Environ.*, *110*(2), 262–274, doi:10.1016/j.rse.2007.02.025.
Stisen, S., I. Sandholt, A. Norgaard, R. Fensholt, and K. H. Jensen (2008), Combining the triangle method with thermal inertia to estimate regional evapotranspiration—Applied to MSG-SEVIRI data in the Senegal River basin, *Remote Sens. Environ.*, *112*(3), 1242–1255, doi:10.1016/j.rse.2007.08.013.
Su, Z. (2002), The Surface Energy Balance System (SEBS) for estimation of turbulent heat fluxes, *Hydrol. Earth Syst. Sci.*, *6*(1), 85–99, doi:10.5194/hess-6-85-2002.
Sun, D., R. T. Pinker, and J. B. Basara (2004), Land surface temperature estimation from the next generation of geostationary operational environmental satellites: GOES MQ, *J. Appl. Meteorol.*, *43*(2), 363–372, doi:10.1175/1520-0450(2004)043<0363:LSTEFT>2.0.CO;2.
Sun, J., G. D. Salvucci, D. Entekhabi, and L. Farhadi (2011), Parameter estimation of coupled water and energy balance models based on stationary constraints of surface states, *Water Resour. Res.*, *47*, W02512, doi:10.1029/2010WR009293.
Sun, J., G. D. Salvucci, and D. Entekhabi (2012), Estimates of evapotranspiration from MODIS and AMSR-E land surface temperature and moisture over the Southern Great Plains, *Remote Sens. Environ.*, *127*, 44–59, doi:10.1016/j.rse.2012.08.020.
Tang, B.-H., Y. Bi, Z.-L. Li, and J. Xia (2008), Generalized split-window algorithm for estimate of land surface temperature from Chinese geostationary FengYun meteorological satellite (FY-2C) data, *Sensors*, *8*(2), 933–951, doi:10.3390/s8020933.
Tang, R. L., Z.-L. Li, and B. H. Tang (2010), An application of the Ts-VI triangle method with enhanced edges determination for evapotranspiration estimation from MODIS data in arid and semi-arid regions: Implementation and validation, *Remote Sens. Environ.*, *114*(3), 540–551, doi:10.1016/j.rse.2009.10.012.
Tang, R. L., Z.-L. Li, Y. Y. Jia, C. R. Li, X. M. Sun, W. P. Kustas, and M. C. Anderson (2011), An intercomparison of three remote sensing-based energy balance models using Large Aperture Scintillometer measurements over a wheat-corn production region, *Remote Sens. Environ.*, *115*(12), 3187–3202, doi:10.1016/j.rse.2011.07.004.
Tang, R. L., Z.-L. Li, K.-S. Chen, Y. Y. Jia, C. R. Li, and X. M. Sun (2013a), Spatial-scale effect on the SEBAL model for evapotranspiration estimation using remote sensing data, *Agric. For. Meteorol.*, *174*, 28–42, doi:10.1016/j.agrformet.2013.01.008.
Tang, R. L., Z.-L. Li, and X. M. Sun (2013b), Temporal upscaling of instantaneous evapotranspiration: An intercomparison of four methods using eddy covariance measurements and MODIS data, *Remote Sens. Environ.*, *138*, 102–118, doi:10.1016/j.rse.2013.07.001.
Tikhonov, A. N., and V. Y. Arsenin (1977), *Solutions of Ill-Posed Problems*, V. H. Winston, Washington, D. C.

Twine, T. E., W. P. Kustas, J. M. Norman, D. R. Cook, P. R. Houser, T. P. Meyers, J. H. Prueger, P. J. Starks, and M. L. Wesely (2000), Correcting eddy-covariance flux underestimates over a grassland, *Agric. For. Meteorol.*, *103*(3), 279–300, doi:10.1016/S0168-1923(00)00123-4.

Verstraeten, W. W., F. Veroustraete, and J. Feyen (2008), Assessment of evapotranspiration and soil moisture content across different scales of observation, *Sensors*, *8*(1), 70–117, doi:10.3390/s8010070.

Wang, K. C., and R. E. Dickinson (2012), A review of global terrestrial evapotranspiration: Observation, modeling, climatology, and climatic variability, *Rev. Geophys.*, *50*, Rg2005, doi:10.1029/2011rg000373.

Wang, K. C., Z. Q. Li, and M. Cribb (2006), Estimation of evaporative fraction from a combination of day and night land surface temperatures and NDVI: A new method to determine the Priestley-Taylor parameter, *Remote Sens. Environ.*, *102*(3–4), 293–305, doi:10.1016/j.rse.2006.02.007.

Xu, T. R., S. L. Liang, and S. M. Liu (2011), Estimating turbulent fluxes through assimilation of geostationary operational environmental satellites data using ensemble Kalman filter, *J. Geophys. Res.*, *116*, D09109, doi:10.1029/2010JD015150.